

We are IntechOpen, the world's leading publisher of Open Access books Built by scientists, for scientists

6,900

Open access books available

186,000

International authors and editors

200M

Downloads

Our authors are among the

154

Countries delivered to

TOP 1%

most cited scientists

12.2%

Contributors from top 500 universities



WEB OF SCIENCE™

Selection of our books indexed in the Book Citation Index
in Web of Science™ Core Collection (BKCI)

Interested in publishing with us?
Contact book.department@intechopen.com

Numbers displayed above are based on latest data collected.
For more information visit www.intechopen.com



Interaction of Femtosecond Laser Pulses with Solids: Electron/Phonon/Plasmon Dynamics

Roman V. Dyukin, George A. Martsinovskiy, Olga N. Sergaeva, Galina D. Shandybina, Vera V. Svirina and Eugeny B. Yakovlev

Additional information is available at the end of the chapter

<http://dx.doi.org/10.5772/46237>

1. Introduction

Femtosecond lasers bring new opportunities in a variety of technological applications [1] in micro- and nanotechnologies, including electronics, mechanics, medicine and biology. Technologies, based on femtosecond effects, are used, for example, to make light absorbers for solar energy devices [2], for direct fabrication of integrated optical components [3], enhancing performance of photo-electronic devices [4], friction reduction and improvement of mechanical wear resistance [5], surface conditioning of medical implants [6], etc. Further development of the above technologies requires deeper understanding of the physical processes occurring under the ultrashort laser pulse action on different materials.

Changes in the material optical properties under the action of intense radiation represent the key feature of the interaction of laser radiation with condensed media. Dynamics of optical properties of solids under the action of femtosecond laser pulse determines a number of physical effects which are of the great interest for both fundamental science and new applications. In particular, the feedbacks, which are being formed in this case, fundamentally change the properties of condensed matter [7].

During the action of femtosecond pulse on solids the electronic subsystem undergoes intensive photoexcitation while the lattice stays cold. The processes of excitation of the electrons and release of the absorbed energy are spaced in time. High intensity of the laser radiation results in modification of the state of the electron subsystem thus significantly changing the optical properties of the medium [8]. Studies of the femtosecond pulses effects on semiconductors and insulators [9, 10] showed that the concentration of nonequilibrium carriers generated by laser radiation is so high that the surface layer acquires properties of the metals during the pulse.

It was observed experimentally that semiconductors can be disintegrated during the femtosecond laser pulse action [11]. In [11] it was proposed a mechanism of destruction based on the crystal lattice destruction by the electric field resulting from the violation of quasi-neutrality in the irradiated area due to the external electron emission - Coulomb explosion. Conditions for Coulomb explosion occurrence in metals were not found.

The currently used experimental approaches such as femtosecond pump-probe technology [12, 13] and mass-spectroscopy (for example, [14]) provide measurement of integral characteristics, but have limited capability for retrieval of dynamics of the processes. The limitations of the experiment approach are being compensated by extensive use of mathematical modeling, where the fast non-linear processes are simulated in a wide range of the initial data.

Two-temperature model, which is traditionally used to describe the ultrashort laser pulse interaction with matter, has proved its validity in various conditions. The phenomenological two-temperature model of parabolic type was proposed in the 50's of last century by M.I. Kaganov, I.M. Lifshitz, L.V. Tanatarov [15]. It has been used by S.I. Anisimov to describe transient phenomena in a nonequilibrium electron gas and lattice under the submicrosecond laser action [16]. The model represents the primary approach to mathematical description of the nonequilibrium heating of the condensed medium by the action of short- and ultrashort-pulse laser radiation. According to the model it is assumed that the energy absorbed by free electrons increases their temperature, then the interaction of the heated electrons with the lattice results in increasing lattice temperature. Heat transfer takes place through the heat conduction mechanisms.

When analyzing the effect of femtosecond laser pulses on matter one has to consider the following: applicability of two-temperature model to description of the electron temperature, which is determined by the electron equilibrium and applicability of the notion of temperature; and taking into account multi-quantum effects in description of electron emission.

The applicability of a two-temperature model for description of action of femtosecond laser pulse on metals. Femtosecond pulse action on the metal can be generally described as follows. Absorption of photons by free electrons in metals results in increase in the electron kinetic energy and the energy distribution becomes nonequilibrium. This well-known feature determines the behavior of metals in a wide spectral range. One can use the diffusion approximation for obtaining qualitative characterization of photoexcitation of solids during the action of femtosecond pulse. With this approach the distribution of free electrons is described by the integral concentration $n(z, t)$, which varies in time and space (along the axis z , directed into the material) due to photo- and thermionic emission from the surface layers and electron diffusion. It is assumed that the thermalization of the electron gas occurs so fast that the notion of electron temperature can be immediately applied. "Hot" electrons contribute to the photo- and thermal emission: they withdraw a part of the energy stored in the electronic subsystem, thus reducing its temperature and, eventually, the temperature of solid as a whole. At the same time, change in the electrons concentration in the surface region results in a change in the optical characteristics of the material.

It is known that the light is absorbed by the conduction electrons in metals. Depending on the concentration of conduction electrons n and the wavelength of the incident light λ the electrons can be considered as free provided $n \gg 1/\lambda^3$, and the free electron model cannot be applied if $n \ll 1/\lambda^3$. In typical conditions in metals, where $n \approx 10^{22} \text{ cm}^{-3}$, and for the light wavelength of $\lambda \approx 1 \mu\text{m}$ the free electron model works well. It is also well known that the electron gas in metals is degenerated at practically all temperature range, and the distribution function of the electron gas just slightly differs from the distribution function at the absolute zero.

The Fermi energy ε_F for metals is very high. For example, for copper $\varepsilon_F = 7.1 \text{ eV}$, for silver $\varepsilon_F = 5.5 \text{ eV}$. For this reason heat effects engage the electrons, whose energy lies in a narrow energy range $\approx 2k_B T$ (k_B - Boltzmann constant) near the Fermi level.

The concentration of electrons, which absorb the incident radiation in metal, can be estimated by using the relation $n = h\nu N / \varepsilon_F$, where ν - the frequency of the incident light. For example, $n/N = 25\%$ of the conduction electrons are affected in copper under $h\nu = 1.7 \text{ eV}$.

The electron transfer part of excessive energy, which they receive due to light absorption, though their collision to other electrons, ions and lattice defects (dislocations, grain boundaries, etc.). Heating of the metal is determined by efficiency of the collisions, which depends on the particles that exchange with energy. Typically the following relation takes place: $\nu_{ee} \gg \nu_{ei} \gg \nu_{ep}$, where ν_{ee} - the frequency of electron - electron collisions, ν_{ei} - the frequency of collisions between electrons and phonons, ν_{ep} - the frequency of electrons collisions with impurities and defects in the metal. The electron-phonon mechanism is quite feasible, since the Fermi energy of electrons in metals is high and is essentially represented by the energy of translational motion of free electrons. The Fermi velocity is $v_F = (2\varepsilon_F/m_e)^{1/2} = 1.5 \cdot 10^8 \text{ cm/s}$ is also high compared to the speed of sound in metals, that is typically: $v_F \sim 10^5 \text{ cm/s}$.

A single collision may not be enough for the electron, which absorbed a photon, to release the excessive energy, i.e. energy relaxation is a multi-stage process of a diffusion character. For this reason, the energy redistribution occurs not only at the skin layer ($\delta_s \sim 10^{-6} \text{ cm}$), but in the deeper layer of $l_d = (D/\nu_{ee})^{1/2} = 10^{-5} \text{ cm}$, where D is the electron diffusion coefficient.

Thus there is a heating of the metal. The heat, which is released in the layer l_d , is further transferred depthward into the material through heat conduction. The characteristic time of the absorbed energy transfer in metal is

$$\tau_{ei} = 1/\nu_{ei} = 10^{-12} - 10^{-11} \text{ s.}$$

The electron gas and the lattice of the metal are two weakly interacting subsystems. Under the conditions:

$$t \gg \tau_{ee}, \quad (1)$$

(τ_{ee} - time to establish an equilibrium energy distribution in the electron gas) and

$$\nu_{ii} \ll \nu_{ei}, \quad (2)$$

(ν_{ii} – frequency of ion-ion collisions) the electron gas and the lattice can be described separately with electron T_e and lattice T_i temperatures. Condition (1) infers rapid redistribution of the absorbed energy between the conduction electrons, and (2) means that the energy transferred to the lattice by electrons, rapidly redistributes between the ions.

Let us excessively consider the relaxation rates ν_{ef} , ν_{ee} , ν_{ei} , ν_{ii} . The relations between these relaxation rates substantially determine the processes in metals during the absorption of radiation.

The frequency of collisions between electrons and photons ν_{ef} is proportional to the power density of laser radiation q absorbed by the metal. It can be estimated using the relation:

$$\nu_{ef} = \frac{\alpha q}{h\nu n}, \quad (3)$$

where α is the absorption coefficient in metals: $\alpha \sim 10^5 \text{ cm}^{-1}$.

The frequency of electron-electron collisions ν_{ee} in the metal is mainly determined by the number of electrons in the Fermi smearing and is calculated using the relation:

$$\nu_{ee} = v_F \sigma_{ee} n_e \left(\frac{k_B T_e}{\varepsilon_F} \right)^2, \quad (4)$$

where v_F – the electron velocity on the Fermi surface $\sim 10^8 \text{ cm/s}$; σ_{ee} – electron - electron interaction cross-section, $\sigma_{ee} \approx 5 \cdot 10^{-16} \text{ cm}^2$; $k_B T_e$ – Fermi smearing region. Then, at $T_e \sim 10^3 \text{ K}$, the value of $\nu_{ee} \approx 10^{14} \text{ s}^{-1}$, and the time to establish an equilibrium distribution of the electron gas $\tau_{ee} \sim 1/\nu_{ee} \sim 10^{-14} \text{ s}$. The rate of energy transfer from the electron gas to the lattice and the lattice temperature is determined by the heat source and heat transfer coefficient of the electrons with the lattice β_{ei} .

The energy, which the lattice obtains from the electron gas per unit volume per unit time is $\sim \beta_{ei}(T_e - T_i)$, $\beta_{ei} \sim 10^{10} \text{ W}/(\text{cm}^3 \text{K})$.

The frequency of electron-ion relaxation can be expressed in terms of heat transfer coefficient

$$\nu_{ei} = \frac{\beta_{ei}}{\rho_i c_i}, \quad (5)$$

where $\rho_i c_i$ – the volumetric heat capacity of the lattice [$10^{-7} \text{ W}\cdot\text{s}/(\text{cm}^3 \text{K})$]. Substituting numerical values one obtains $\nu_{ei} \sim 10^{11} \text{ s}^{-1}$ and $\tau_{ei} \sim 10^{-11} \text{ s}$.

Comparing the expressions (3) and (4), one can show that (1) is always satisfied with the flux densities $q_0 \leq 10^9 \text{ W}/\text{cm}^2$ and the electron gas in a metal is described by temperature T_e . Similarly, the condition (2) is also satisfied, therefore temperature T_i can be introduced to describe the thermal state of the lattice.

Thus, the electron relaxation time is estimated as $\tau_r \sim 1/\nu_{ee}$, where ν_{ee} – the frequency of electron-electron collisions. According to the estimates given above, its magnitude is about

10^{-14} – 10^{-13} s, which is comparable with the pulse duration (tens of femtoseconds). However, further studies [16-19] have shown that the electron-electron relaxation time can be reduced up to 10^{-16} s at the electron gas temperatures of $\sim 100\,000$ K, achieved by the action of ultrashort laser pulse. In other words, two-temperature model could be applied to analyze the effects of femtosecond laser pulse.

Multiphoton absorption. Although the theory of multiphoton absorption is pretty well developed [17], there is a certain difficulty regarding definition of multi-photon absorption cross-sections of real media, when this theory is used for the analysis of multiphoton absorption during femtosecond laser action.

In terms of quantum mechanics multiphoton process can be represented as a series of successive transitions of an electron to the virtual states [18]. Only the initial and final states are real in this case. The energy conservation law is valid with an accuracy of a natural width of the energy level only for the initial and final states. For virtual states the energy conservation law takes place with the accuracy, that is determined by the energy-time uncertainty relation $\delta E \cdot \delta t \geq \hbar$. At each virtual state the quantum system lives for the time:

$$\delta t \geq \hbar / \delta E. \quad (6)$$

Absorption of another photon makes the system transit to the next state.

It means that the quantum system can potentially absorb a photon of any energy, however the lifetime of the quantum system, absorbing a photon, would differ. If the quantum system absorbs a photon with energy $h\nu = \Delta E_{mn}$, the system transits into a real state, where the lifetime δt is determined by the probability of spontaneous decay of this state. If the quantum system absorbs photon with energy $h\nu \neq \Delta E_{mn}$, the system transits into a virtual state, where the lifetime is determined by the energy-time uncertainty relation: $\delta t \geq \hbar / \delta E$, $\delta E = |h\nu - \Delta E_{mn}|$.

With this approach one can use the following method for estimation of multiphoton absorption cross sections for various medium. One-photon absorption cross section σ_1 for metals can be determined by the known absorption coefficient α and the concentration of free electrons n : $\sigma_1 = \alpha / n$. Estimating the lifetime of an electron on a virtual level with the photon energy of about 1 eV $\tau_0 \sim 10^{-16}$ s and assuming the absorption cross section of excited electrons in all virtual levels to be equal to σ_1 , one obtains two-photon absorption cross section to be $\sigma_2 = \sigma_1^2 n \tau_0$. Similar consideration provides $\sigma_3 = \sigma_1^3 n \tau_0^2$. Consequently for $m+1$ -photon absorption cross section is $\sigma_{m+1} = \sigma_1^{m+1} n \tau_0^m$. For example, for $\alpha = 10^5 \text{ cm}^{-1}$ and $n = 10^{22} \text{ cm}^{-3}$ one can obtain $\sigma_1 = 10^{-17} \text{ cm}^2$, $\sigma_2 = 10^{-28} \text{ cm}^2 \text{ s}$, $\sigma_3 = 10^{-61} \text{ cm}^3 \text{ s}^2$.

2. Effect of electron emission on metal heating and destruction by femtosecond laser pulse

Let us analyze the influence of hot electron emission on heating and destruction of metals based on a two-temperature model and using as example the numerical simulation of Coulomb explosion.

In theoretical studies dealing with the different variants of two-temperature model, the most important aspect is to define the nonlinear optical and thermal properties in a wide temperature range, as well as quantitative characteristics of the electron-electron and electron-phonon interaction, controlling the temperature of the electron gas and the energy exchange between electrons and lattice, respectively.

In terms of the numerical analysis classical version of a two-temperature model is a system of interrelated differential equations of heat conduction, the accuracy of whose solution depends strongly on adaptation of the computational grid to the required numerical solution.

Let us consider the two-temperature model of metal heating by a femtosecond laser pulses on metals [19-22]. The model consists of a system of heat-conduction equations for the electrons and the phonons (lattice) subsystems, where thermophysical properties depend on electron temperature T_e and electron concentration n , and the equation describing the temporal evolution of the electron concentration.

$$c_e(T_e, n) \frac{\partial T_e}{\partial t} - \frac{\partial}{\partial z} \left[\lambda_e(T_e, n) \frac{\partial T_e}{\partial z} \right] = -\beta_{ei}(T_e, n)(T_e - T_i) + q_v, \quad (7)$$

$$c_i \frac{\partial T_i}{\partial t} - \frac{\partial}{\partial z} \left[\lambda_i \frac{\partial T_i}{\partial z} \right] = \beta_{ei}(T_e, n)(T_e - T_i), \quad (8)$$

where λ_e , λ_i , c_e , c_i are the electron and lattice heat conductivity and heat capacity, β_{ei} – electron-ion energy transfer coefficient, q_v – the absorbed power density released in the electron subsystem.

Dependence of optical and thermo-physical properties of metal [23] on the electron temperature and concentration is taken into account for electron heat capacity:

$c_e = \frac{\pi^2 k_b^2 n(z, t) T_e}{2 \varepsilon_F}$, electron heat conductivity: $\lambda_e = v_e^2 \tau_{ee} c_e / 3$, electron-ion energy transfer

coefficient: $\beta_{ei} = c_e / t_{ei}$, electron velocity: $v_e = \sqrt{3 k_b T / m_e}$, the electron mean free path: $l_e = 1 / (n \sigma \sqrt{2})$. The absorption coefficient of metals depends only on the concentration of free electrons: $\alpha(n) = (\alpha / n_0) n$, n_0 is the initial concentration of free electrons.

The boundary conditions:

$$\lambda_e \frac{\partial T_e}{\partial z} \Big|_{z=0} = -j_e, \quad \lambda_i \frac{\partial T_i}{\partial z} \Big|_{z=0} = 0, \quad T_e \Big|_{z=\infty} = T_i \Big|_{z=\infty} = T_n,$$

where j_e – is the heat flow carried away by the emitted electrons, T_n – the initial temperature. Evolution of the electron density distribution is described by the following diffusion equation:

$$\frac{\partial n(z, t)}{\partial t} = D \frac{\partial^2 n(z, t)}{\partial z^2}, \quad (9)$$

with initial and boundary conditions:

$$D \frac{\partial n}{\partial z} \Big|_{z=0} = -F_e, \quad n \Big|_{z=0} = n_0, \quad n \Big|_{z=\infty} = n_0,$$

where $n_0=10^{22} \text{ cm}^{-3}$ is the initial concentration of electrons evenly distributed over the volume, F_e is the flow of the electrons resulted from thermionic emission and photoemission $F_e=F_t+F_{mphoto}$.

The thermionic emission is determined by the law of Richardson:

$$F_t = -BT_e^2 \Big|_{z=0} \exp\left(-\frac{\phi_e}{k_b T_e \Big|_{z=0}}\right) \exp(-z/l_e) / q_e,$$

here B is the Richardson coefficient, ϕ_e is the work function, q_e is the electron charge.

External photoelectric effect implies that the energy of absorbed photons is used by the electrons to overcome the work function, i.e. the minimum energy required for the electron to escape from the surface. The work function in metals is several eV (for silver $\phi_e=4,28$ eV). Therefore, for $h\nu=1.55$ eV one should expect the three-photon absorption. For calculating the photoemission let us assume that the free electrons, which are involved into the multiphoton process, reach the surface without energy loss and leave the metal. The emissive layer thickness is limited by the electron mean free path and also depends on the electron concentration and the emission coefficient. The flow of electrons (cm^{-2}/s) caused by photoemission for the m -photon absorption:

$$F_{mphoto} \Big|_{z=0} = -\int_0^{\infty} \sigma_m J^m \exp(-z/l_e) dz,$$

J is the absorbed photons flow, $J=q/h\nu$, σ_m is the multi-photon absorption cross section.

The emission of electrons leads to accumulation of positive charge on the metal surface and, therefore, to generation of the electric field. The electric field resulted from breaking of quasi-neutrality of the irradiated area can be calculated from the following equation [24]:

$$\frac{\partial E}{\partial z} = \frac{q_e}{\epsilon \epsilon_0} (n_i - n). \quad (10)$$

This electric field, which is induced by the charge separation, can reach extremely high magnitude and exceed the energy of atomic bonds resulting in Coulomb explosion. To determine the conditions for initiation of the Coulomb explosion the electric field (10) is compared to the threshold magnitude required for removal of an atom from the target. The estimation of the critical electric field [24]:

$$E_{th} \Big|_{z=0} = \sqrt{\frac{2\Lambda n}{\epsilon \epsilon_0}},$$

where n_0 - the concentration of atoms (cm^{-3}), $\Lambda = 2.951 \text{ J/atom}$ - the heat of sublimation, $\varepsilon = 4.9$ - relative permeability of silver, $\varepsilon_0 = 8.854 \cdot 10^{-14} \text{ F/cm}$ - dielectric constant.

For the numerical solution of the heat conduction equation and the equation describing the electron density, which are non-stationary partial differential equations, the finite difference method was applied. To calculate the values of the temperature and the electron concentration explicit difference scheme was used. Though explicit scheme provides a relatively high speed of calculation, it has a serious disadvantage related to the need for satisfying the stability conditions, which impose limits on the amount of steps partitions with respect to coordinate and time.

Fig. 1 - 4 show the results for silver for the laser pulse shape $q = q_m \exp(-(t-t_m)^2/t_{m1}^2)$, $t_m = 100 \text{ fs}$, $t_{m1} = 50 \text{ fs}$. The calculation was performed until the beginning of the Coulomb explosion, when the electric field resulted from the charge separation exceeds the threshold required for the removal of atoms. For comparison, the simulation was performed without taking the emission into account, but preserving the dependence of material properties on temperature.

Fig. 1 shows that temperature of the electrons and the lattice increase, but does not reach its maximum during the pulse. The difference between the temperature, calculated taking into account the emission and without it at the beginning of Coulomb explosion $t = 0.15 \text{ fs}$ is $\Delta T \approx 290 \text{ K}$ for temperature of the electrons (Fig. 1b) and $\Delta T \approx 60 \text{ K}$ for temperature of the lattice.

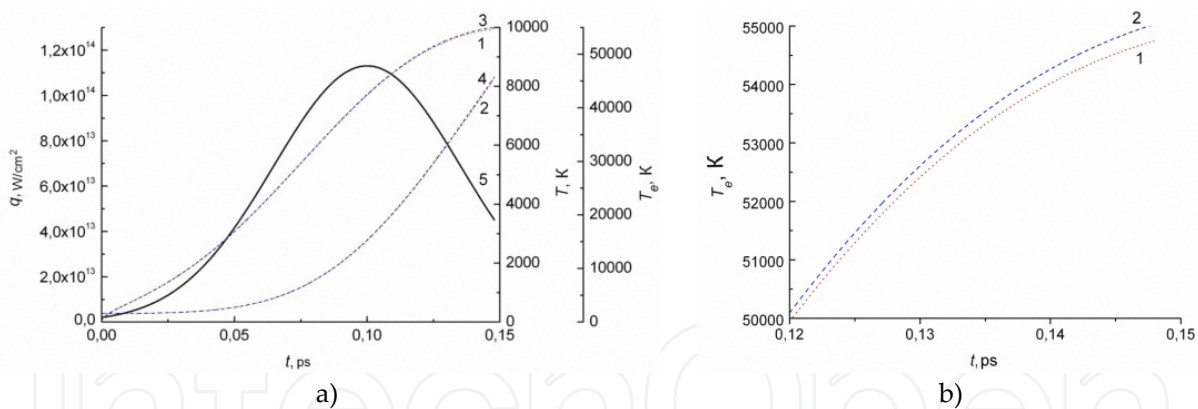


Figure 1. a – Transient behavior of electron and lattice temperature: (1) and (2) – with taking into account emission, (3) and (4) – disregarding emission. (5) – laser pulse shape $q = q_m \exp(-(t-t_m)^2/t_{m1}^2)$, $t_m = 100 \text{ fs}$, $t_{m1} = 50 \text{ fs}$, maximum power density $q_m = 5 \cdot 10^{14} \text{ W/cm}^2$. b – an enlarged part of the temporal dependence of the electron temperature: (1) – with taking into account emission, (2) – disregarding emission

Fig. 2, 3 illustrate temporal behavior of the free electrons concentration, and the number of electrons emitted by photo- and thermionic emission for different pulse shapes. At the initial stage of pulse action photoemission dominates, but thermionic emission increases with the electron temperature rapidly, so thermionic emission begins to prevail over the photoemission. The maximum of the photoemission rate maximum corresponds to the maximum of laser power density. This indicates that the laser pulse shape significantly influences the dynamics of the processes.

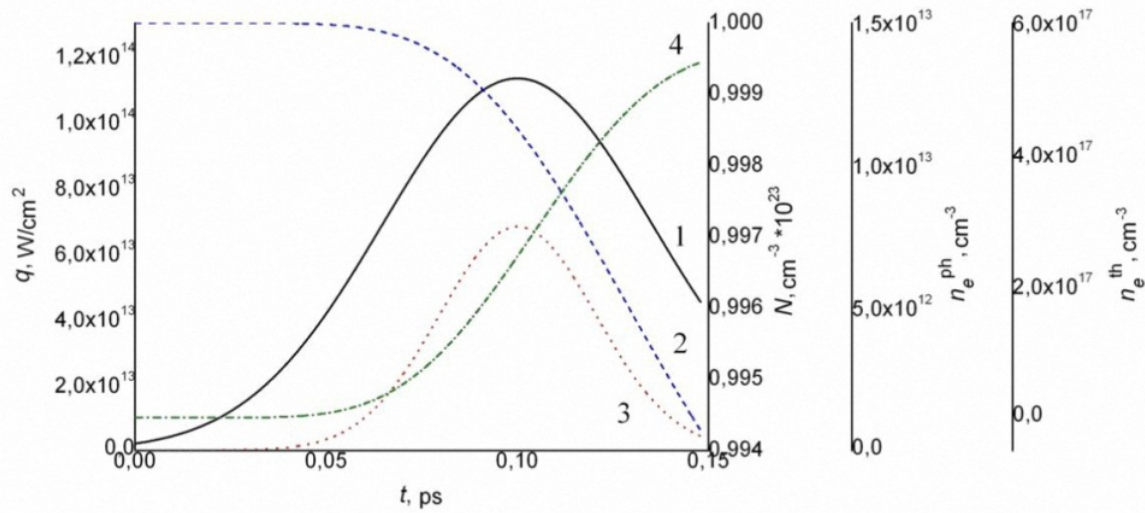


Figure 2. Laser pulse shape (1), the temporal evolution of the net surface electron density N (2) and the density of emitted electrons due to photoemission n_e^{ph} (3) and thermionic emission n_e^{th} (4). Laser pulse shape $q=q_m \exp(-(t-t_m)^2/t_{m1}^2)$, $t_m=100$ fs, $t_{m1}=50$ fs

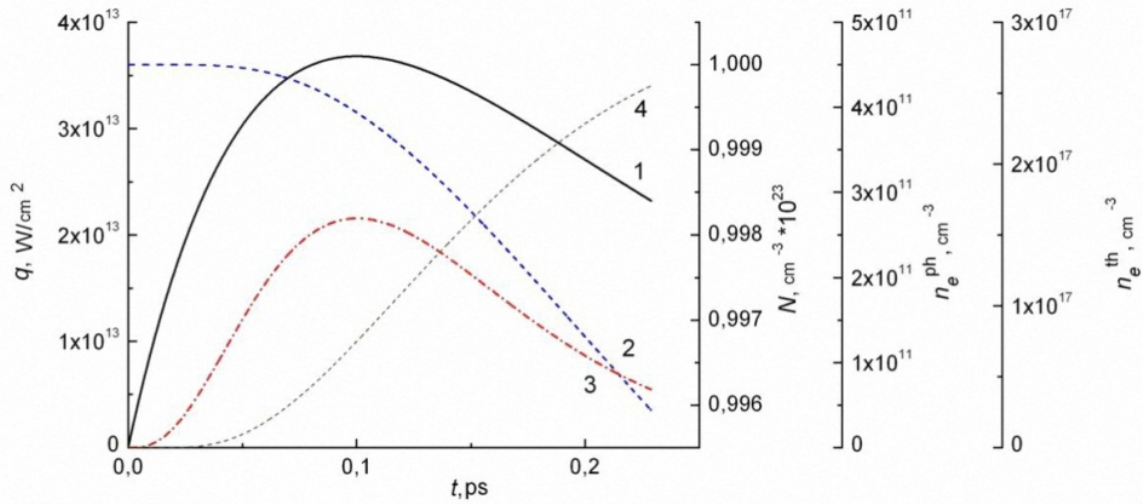


Figure 3. Laser pulse shape (1), the temporal evolution of the net surface electron density N (2) and the density of emitted electrons due to photoemission n_e^{ph} (3) and thermionic emission n_e^{th} (4). Laser pulse shape $q=q_m(t/t_m)\exp(-t/t_m)$, $t_m=100$ fs

The gradient of the electron density results in an electric field, which grows and reaches the Coulomb explosion threshold (Fig. 4).

Fig. 5 illustrates the nonlinear dependence of the moment when Coulomb explosion starts on the laser power density. It is seen that the dependence is nonlinear, and Coulomb explosion for a pulse duration ~ 100 fs can occur when $q > 10^{15}$ W/cm².

We can draw the following conclusions from the results of numerical simulation of the influence of electron emission on heating and destruction of metals irradiated by femtosecond laser pulse.

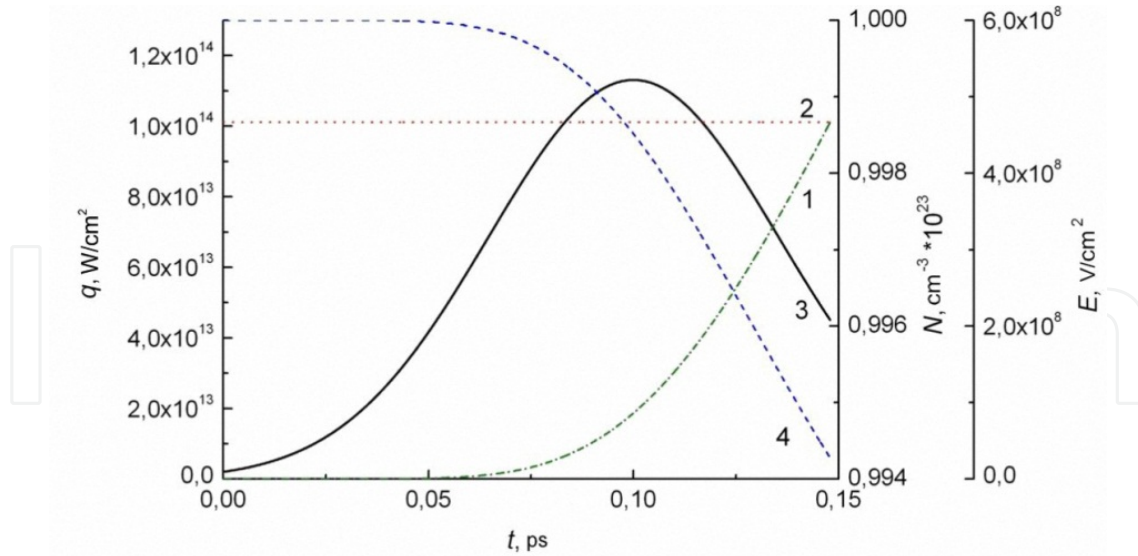


Figure 4. Temporal dependence of the electric field E (1), arising due to emission of electrons and the threshold field value E_{th} (2) corresponding to the beginning of Coulomb explosion. Laser pulse shape $q=q_m \exp(-(t-t_m)^2/t_{m1}^2)$, $t_m=100$ fs, $t_{m1}=50$ fs (3) and the temporal evolution of the net surface electron density (4)

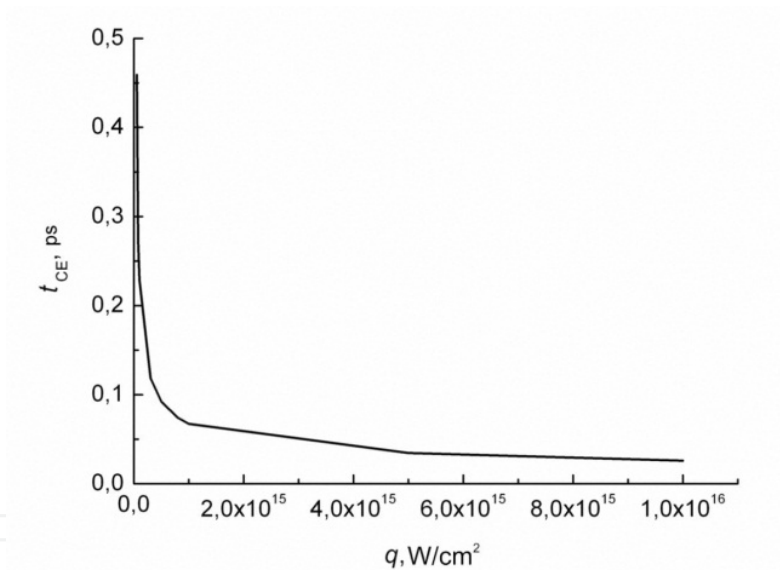


Figure 5. Time of Coulomb explosion onset as function of laser density for laser pulse shape $q=q_m \exp(-(t-t_m)^2/t_{m1}^2)$, $t_m=100$ fs, $t_{m1}=50$ fs

Various types of emission have different impacts on the concentration of emitted electrons (see Fig. 2-3): thermionic emission dominates over the photoemission and increases with the electron temperature increasing. The pulse shape significantly affects on the dynamics of the emission processes. However, according to the calculations the effect of emission processes on the electron gas temperature and the lattice temperature (Fig. 1a, b) is negligible. Also, numerical experiment showed that the occurrence of Coulomb explosion (caused by the emission processes during the pulse) in metals requires high-power incident radiation, which is impossible in the real exposure modes.

Emission processes have a significant impact on the processes of heating and destruction of the semiconductors, because the initial concentration of conductivity electrons in semiconductors can be below concentration of free electrons generated by the action of femtosecond laser radiation in contrast to metals. Let us consider the emission impact on the example of a femtosecond microstructuring of the silicon surfaces.

3. Effect of electron emission on changes in optical properties of semiconductors under the femtosecond laser pulse action

The formation of periodic surface structures (PSS) is a perfect evidence of an induced change in the surface optical properties under the femtosecond pulse action on semiconductor and wide-band dielectrics (Fig. 6). Being formed under different conditions PSS exhibit the same formation regularities: the structures orientation depends on the direction of polarization vector of the laser radiation; the structures period depends on the wavelength, incidence angle of the radiation and dielectric permeability of the medium. The observed regularities suggest that the mechanism of PSS formation is determined by electromagnetic field, which is the result of interference of the incident wave and the excited surface electromagnetic waves (SEW).

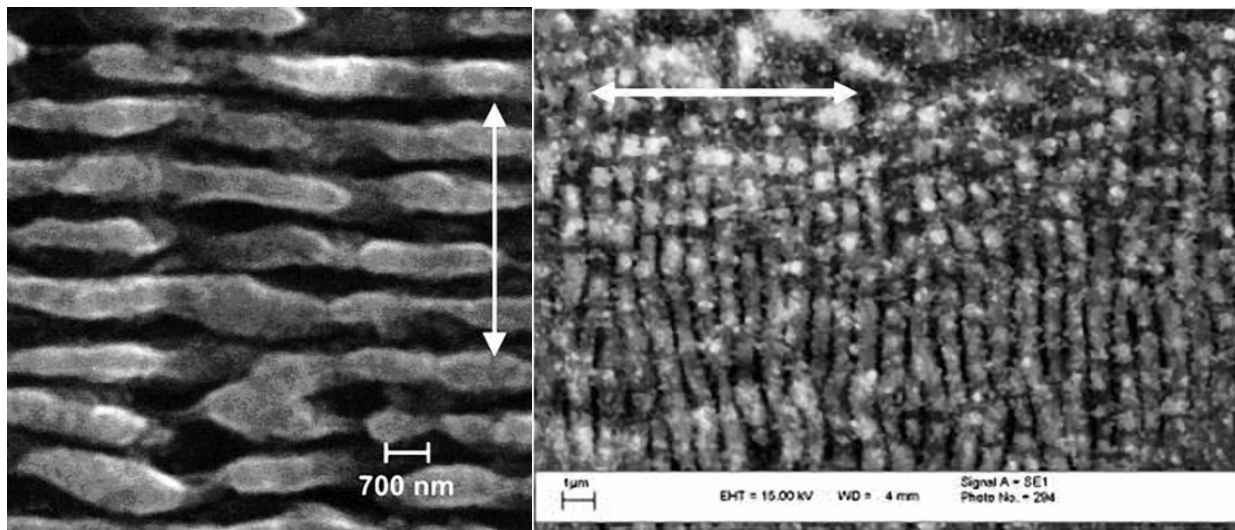


Figure 6. SEM image of the monocrystalline silicon surface irradiated by the laser pulse. Arrow indicates the direction of laser radiation polarization. Left: after irradiation by 1200 pulses, the energy density is $\sim 1 \text{ J/cm}^2$. Right: after exposure by 300 pulses, the energy density is $\sim 2 \text{ J/cm}^2$

Microstructures shown in Fig. 6, were obtained on silicon irradiated by 80 fs laser pulses at a wavelength of $1.25 \mu\text{m}$ [25, 26]. Surface structures turned during rotation of the laser radiation polarization vector, and depending on the density of laser flux were oriented either perpendicular ($Q_0 \sim 1 \text{ J/cm}^2$) or parallel to the direction of polarization ($Q_0 \sim 2 \text{ J/cm}^2$).

It should be noted that low concentration of free electrons in semiconductor in the initial state does not provide the surface optical properties, which are necessary for excitation of

the SEW. In case of longer laser pulses (longer than tens of picoseconds) experimentally observed excitation of SEW on semiconductors is related to properties of the melt formed on the surface due to laser heating. This explanation can't be used for femtosecond action because photoexcitation and thermal processes are separated in time and the surface does not melt during the laser pulse. The conditions for excitation of SEW during ultrashort laser pulse result from high concentration of nonequilibrium carriers, which are generated in the semiconductor by the light.

Dynamics of the optical properties change at the surface of semiconductors under femtosecond laser action is related to change of the non-equilibrium carriers plasma frequency. In order to analyze the behavior of the optical properties let us first consider the basic mechanisms of light absorption and recombination of the absorbed energy.

Total absorption coefficient in semiconductors can be considered as a sum of absorption coefficients associated with different mechanisms $\alpha = \sum_{i=1} \alpha_i$. First of all these are fundamental

band-to-band absorption of light ($h\nu > E_g$, E_g is the band-gap) and intraband absorption, i.e. absorption by free carriers - electrons and holes (from now on we consider only the electrons for simplicity). Rate of relaxation of the crystal electron system from the excited state to the equilibrium state is determined by the recombination mechanisms with characteristic times $\sim 10^{-12}$ - 10^{-10} s.

During femtosecond laser pulse the light intensity can achieve very high level without destruction of the matter, therefore initiating multiphoton processes. In the wavelength range from IR to near UV the energy of a single photon is not sufficient for electron transition from the valence band to the conduction band ($h\nu < E_g$). Such transition takes place as a result of simultaneous absorption of several photons. In this case the rate (or probability) of multiphoton ionization is highly dependent on the laser power. The multiphoton ionization rate is proportional to σI^m , where I is the laser radiation intensity, σ_m - m -photon absorption cross-section. The required number of photons is determined by the lowest value of m , satisfying the relation $m h\nu > E_g$.

During femtosecond laser pulse only photoexcitation and fast electronic processes are observed, while recombination and lattice heating can be neglected, because the characteristic times of these processes are much higher than the pulse duration. This is one of the major differences between action of ultrashort and longer laser pulses.

Model. According to the model the dynamics of distribution of nonequilibrium electron concentration $n(z, t)$ during the femtosecond pulse is determined by generation of the nonequilibrium electrons due to two-photon absorption ($h\nu < E_g$) followed by their diffusion and participation in collision processes as described in the diffusion equation (11).

In this consideration nonequilibrium electrons are the electrons that transit from the valence band to the conduction band under photo-excitation, and then contribute to increasing electron gas temperature, emission, and finally recombination after the end of the pulse. Below by "electrons" we will understand "non-equilibrium electrons" and by "electron gas" we will understand "nonequilibrium electrons gas".

$$\frac{\partial n(z,t)}{\partial t} = \alpha_{2phi} J + D \frac{\partial^2 n(z,t)}{\partial z^2} - \frac{n(z,t)}{\tau_e}, \quad (11)$$

where D is the diffusion coefficient of electrons in a solid, τ_e is the time of electron collisions.

Similarly to the above considerations for metals, the losses of electrons at the surface caused by external emission are taken into account in the model as follows:

$$-D \frac{\partial n(z,t)}{\partial z} \Big|_{z=0} = F_{2pho} \Big|_{z=0} + F_t \Big|_{z=0}, \quad (12)$$

$$F_{2pho} \Big|_{z=0} = - \int_0^{\infty} \sigma_2 J^2 \exp(-z/l_e) dz. \quad (13)$$

Expression (13) describes two-photon emission. Single-photon absorption cross-section σ_1 is estimated assuming the maximum absorption coefficient, that corresponds to absorption by free carriers in metal $\sigma_1 \approx \alpha_{max}/n_{max} \sim 10^{-17} \text{ cm}^2$ (n_{max} is electron concentration in the metal). Photo-ionization of atoms is considered in terms of electron transition through virtual states. The electron life time (τ_0) at these virtual states is determined basing on the uncertainty relation between energy and time: $\tau_0 \sim 10^{-16} \text{ s}$. In this case two-photon cross-section is given by $\sigma_2 \approx \sigma_1^2 n(z,t) \tau_0 \sim 10^{-28} \text{ cm s}$. Expression (14) describes external thermo-emission (Richardson low).

$$F_t = -BT_e^2 \Big|_{z=0} \exp\left(-\frac{\phi_e}{k_b T_e \Big|_{z=0}}\right) \exp(-z/l_e) / q_e \quad (14)$$

Temperature of electrons gas (T_e) is determined by heat conduction equations (15), where heat capacity of electron gas is a function of temperature and concentration.

$$\begin{aligned} \frac{\partial T_e}{\partial t} &= a_e \frac{\partial^2 T_e}{\partial z^2} - \beta_{ei} (T_e - T_i) / c_e + \alpha_e J h \nu / c_e, \\ \frac{\partial T_i}{\partial t} &= a_i \frac{\partial^2 T_i}{\partial z^2} - \beta_{ei} (T_e - T_i) / c_i, \end{aligned} \quad (15)$$

$$c_e = \frac{\pi^2 k_b^2 n(z,t) T_e}{2 \mathcal{E}_F}, \quad (16)$$

where F_{2pho} is determined from (13) for two-photon photoeffect, F_t - from (14).

The Bouguer–Lambert differential law of Eq. (17) determines the intensity distribution $J(z, t)$ inside the solid (the z axis is directed depth ward). In this model absorptance of the material (A) is assumed to be constant.

$$\begin{aligned}
\frac{\partial J(z,t)}{\partial z} &= -(\alpha_{2phi} + \alpha_e + \alpha_{2pho})J(z,t), \\
J(0,t) &= AJ_0(t); J_0(t) = q_0(t) / (h\nu), \\
q_0(t) &= q_m(t/t_m)\exp(-t/t_m),
\end{aligned}
\tag{17}$$

where $AJ_0(t)$ is the density of the absorbed photon flux, with a bell-shaped temporal distribution of intensity of the laser radiation, α_{2phi} is two-photon absorption coefficient of the inner photoeffect, α_{2pho} is two-photon absorption coefficient of the extrinsic photoeffect, and α_e is coefficient for absorption by free electrons, which in turn are defined as

$$\begin{aligned}
\alpha_{2phi} &= \sigma_1^2 n_{\max} \tau_v J, \\
\alpha_{2pho} &= \sigma_1^2 n(z,t) \tau_v J, \\
\alpha_e &= \sigma_1 n(z,t).
\end{aligned}
\tag{18}$$

Expressions (11-18) along with initial and boundary conditions at $t = 0$ and $z = \infty$

$$\begin{aligned}
n|_{z=\infty} &= n|_{t=\infty} = 0, \\
T_e|_{z=\infty} &= T_i|_{z=\infty} = T_e|_{t=0} = T_i|_{t=0} = 0
\end{aligned}
\tag{19}$$

allow one to obtain spatial and temporal distribution of the electron concentration in semiconductor $n(z, t)$.

The first qualitative estimates were made for a simplified model, in which the emission mechanism is generalized and the emission flux in the expression (12) is taken into account using the emission factor μ without separation of photo- and thermal emission

$$-D \frac{\partial n(z,t)}{\partial z} \Big|_{z=0} = -\mu n.$$

Fig. 7 shows obtained variation of the electron concentration with depth during the laser pulse action on silicon. The following initial data were used for the calculation: $D = 80 \text{ cm}^2/\text{s}$, $\tau_e = 10^{-14} \text{ s}$, $\mu = 2 \cdot 10^8 \text{ cm/s}$, $Q_0 = 2 \text{ J/cm}^2$, pulse duration is 80 fs, wavelength is 1.25 μm . The calculation results indicate that the semiconductor surface acquires properties of a metal during the laser pulse action. The maximum of electron density is located at some distance from the surface. It shifts from the surface into the bulk of material and its value increases during the pulse action. By the middle of the pulse the distribution of electron concentration stabilizes following the shape of the laser pulse.

The above estimates showed that dynamics of the optical properties of semiconductor under action of ultrashort pulse can be described within the same approach used for metals. According to Drude dispersion theory the dielectric permeability of photoexcited semiconductor can be determined by the plasma frequency of the electron gas (ω_p), incident radiation frequency (ω) and the frequency of electron collisions (γ), according to following expressions:

$$\varepsilon = \varepsilon' + i\varepsilon'',$$

$$\text{Re } \varepsilon = \varepsilon_n - \frac{\omega_p^2}{\omega^2 + \gamma^2}, \quad (20)$$

$$\text{Im } \varepsilon = \frac{\omega_p^2 \gamma}{\omega(\omega^2 + \gamma^2)},$$

$$\omega_p = \sqrt{\frac{4\pi n(z,t) q_e^2}{m_e}}, \quad (21)$$

where ε_n is the initial value of the semiconductor permittivity, and ε' and ε'' is the real and imaginary parts of the permeability.

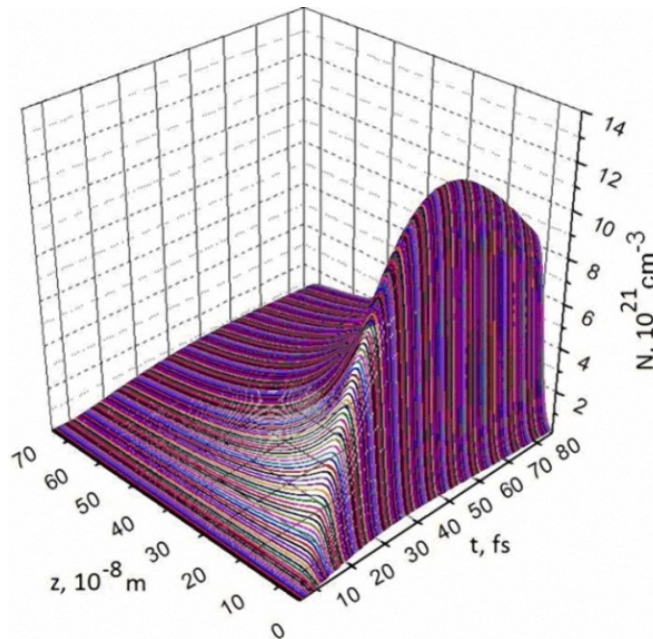


Figure 7. The dynamics of silicon photoexcitation

Let us consider dynamics of the dielectric permeability in the surface layer of semiconductor taking into account the change in the plasma frequency of non-equilibrium carriers by using a mathematical model (11-21). This will help us to identify the role of different emission processes in evolution of the optical properties during a femtosecond pulse.

Numerical simulation was performed for silicon ($\varepsilon_n = 12$, $\gamma = 10^{14} \text{ s}^{-1}$) with initial data given above. The calculation results are shown on Fig. 8-10.

When there is no emission surface the real part of dielectric permeability at the surface quickly decreases and becomes negative stabilizing by the end of the first quarter of the pulse (Fig. 10, curve 1). If external photo-emission is taken into account, the character of the dynamics of $\text{Re } \varepsilon$ does not change, but the magnitude at which the permeability stabilizes is increased (Fig. 8, curve 2). Thermionic emission strongly affects the dynamics of the

permeability. Influence of the thermionic emission is small in the beginning of the pulse and value of $\text{Re}\varepsilon$ abruptly decreases. Few femtosecond later contribution of the thermionic emission grows and value of $\text{Re}\varepsilon$, returned to its initial level after several damping oscillations (Fig. 8, curve 3). The observed inertia is typical for the thermionic emission mechanism, and the return of the dielectric permeability to the initial value means that all the "hot" electrons leave the surface as a result of thermal emission. If photo-emission is also taken into account escape of the electrons speeds up (Fig. 8, curve 4).

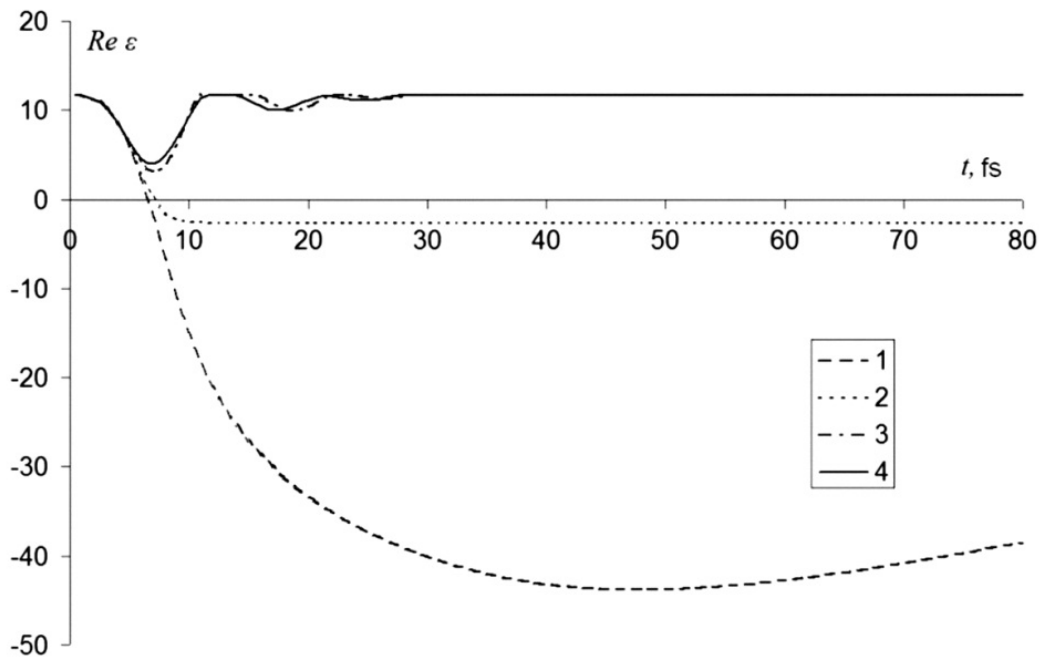


Figure 8. Dynamics of the real part of the permeability at the surface of silicon ($Q_0 = 2 \text{ J/cm}^2$). 1 – no external emission, 2 – only photo-emission is taken into account, 3 – only thermionic emission is taken into account, 4 – combined action of photo-emission and thermal emission

Figure 9 shows dynamics of the real part of the permeability at the silicon surface for different values of the light flux density. If only two-photon photo-emission is taken into account, the surface acquires metal-like properties at the first femtoseconds of the pulse, and the permeability remains negative during the entire pulse. Increasing the radiation-flux density reduces the time to reach the steady-state level without changing the character of the dependence (Fig. 9a). When both photo-emission and thermionic emission are taken into account the picture changes (Fig. 9b). If $Q_0 \leq 1 \text{ J/cm}^2$, $\text{Re}\varepsilon$ smoothly returns to its initial value (curve 1). When the energy density increases the permeability oscillates during transition to its initial value (curves 2 and 3). These oscillations result from dependence of heat capacity of the electron gas on electron concentration. The higher light flux induces higher temperature of the electron gas and contribution of thermionic emission increases. As a result the permeability returns to its initial value faster. At the same time increasing flux density raises the electron concentration and, accordingly, the heat capacity of the electron gas increases thus reducing its temperature and the contribution of the thermal emission. This results in oscillating of dielectric permeability.

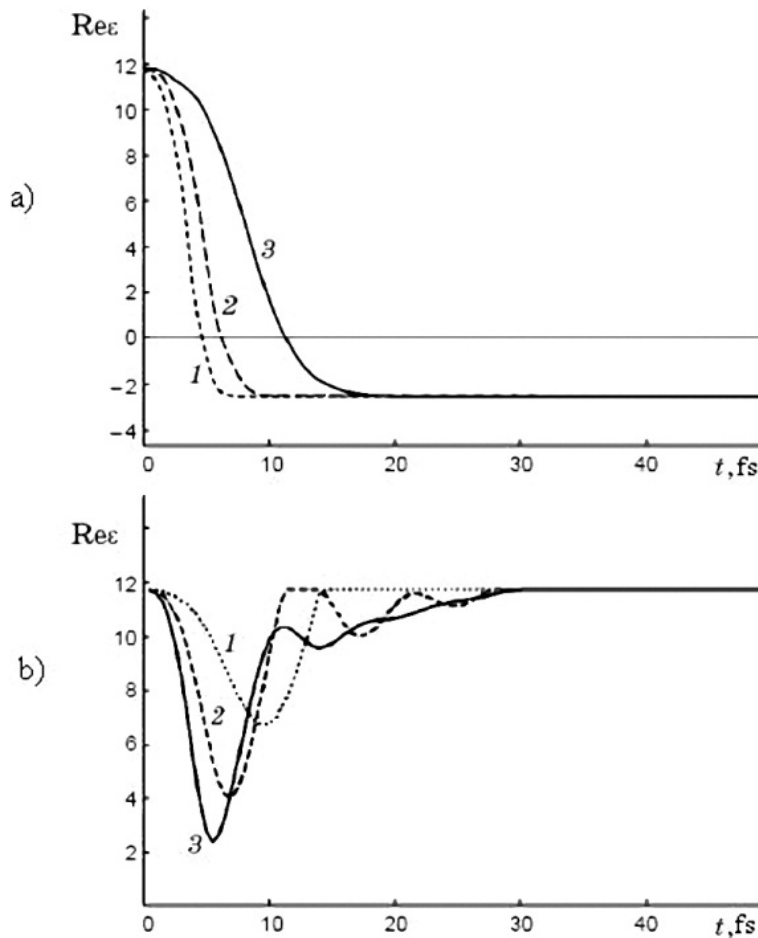


Figure 9. Dynamics of the real part of the permeability on the surface of silicon for various values of the light-flux energy density. (a) Photoemission only, (b) Combined action of photoemission and thermal emission. 1 – $Q_0 = 1 \text{ J/cm}^2$, 2 – $Q_0 = 2 \text{ J/cm}^2$, 3 – $Q_0 = 3 \text{ J/cm}^2$

Figure 10 shows the calculated distribution of permeability $\text{Re}\epsilon(z)$, at the end of the pulse ($Q_0 = 2 \text{ J/cm}^2$). If there is no emission, a very thin metal-like layer appears on the surface (curve 1). If external photo-emission is taken into account, a metal-like layer (several tens of nanometers thick, curve 2) is formed. The loss of the electrons due to thermionic emission qualitatively changes the permeability distribution depth wards (curve 3). A layer with smaller permeability than its initial value is formed at a distance of tens of nanometers from the surface. Combined action of photo-emission and thermionic emission shifts this layer deeper (curve 4).

Let us consider again the conditions necessary for the SEW excitation in order to compare the results of numerical simulation with the above experimental data on femtosecond silicon microstructuring associated with the SEW excitation.

It is known that the formation of PSS oriented perpendicular to the polarization of laser radiation usually results from excitation of surface plasmon-polaritons under the laser pulse action on the metal. Surface plasmon-polaritons are partially longitudinal electromagnetic waves of the TM-type propagating along the interface between two media with the wave electro-magnetic field being localized near the interface. Excitation of plasmon-polaritons is

possible only if one of the media has positive dielectric permeability ($\epsilon_1 > 0$), while the real part of dielectric permeability of the other is negative ($\text{Re}\epsilon_2 < 0$). Also, the condition $|\text{Re}\epsilon_2| > \epsilon_1$ must be satisfied. A negative dielectric permeability in a metal is determined by a high concentration of free electrons. In the case of the relatively long laser pulse action (tens of picoseconds or more) on the semiconductor the appearance of metal-like optical response is usually associated with the properties of the melt formed on the surface due to laser heating.

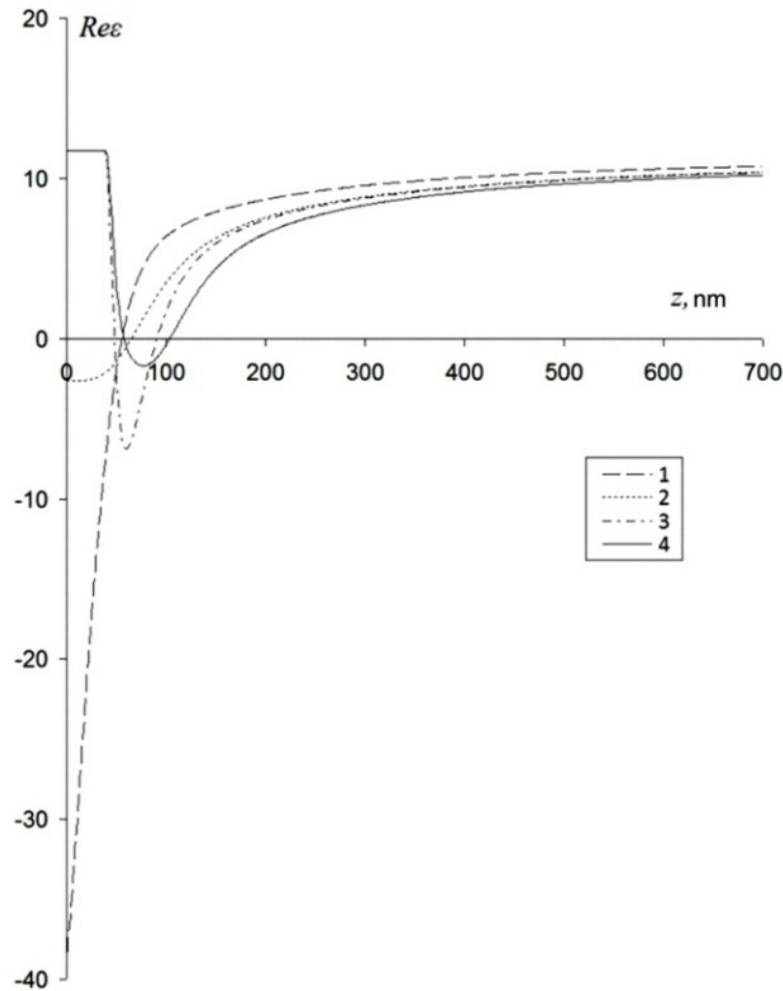


Figure 10. Spatial distribution (into the depthward of the semiconductor) of the real part of the permeability at the end of the laser pulse. 1 – no external emission of electrons, 2 – photo-emission only, 3 – thermionic emission only, 4 – combined action of photo-emission and thermal emission

Semiconductors typically have positive value of their dielectric permeability in the visible and IR range. Under the femtosecond laser pulse action the concentration of nonequilibrium carriers in semiconductors can become so high that dielectric permeability ϵ would change its sign and creates conditions for excitation of surface plasmon-polaritons. In this case, the formation of PSS perpendicular to the polarization vector is experimentally observed.

The formation of structures parallel to the polarization vector is associated with the excitation of surface waveguide modes (TE-polaritons). It is necessary to create an optically layered structure for excitation of a waveguide mode at the semiconductor surface (Fig. 11).

The refractive index of the waveguide layer in such optically layered structure (n_2) exceeds the refractive index values of adjacent layers (n_1, n_3), ($n_2 > n_1, n_2 > n_3$).

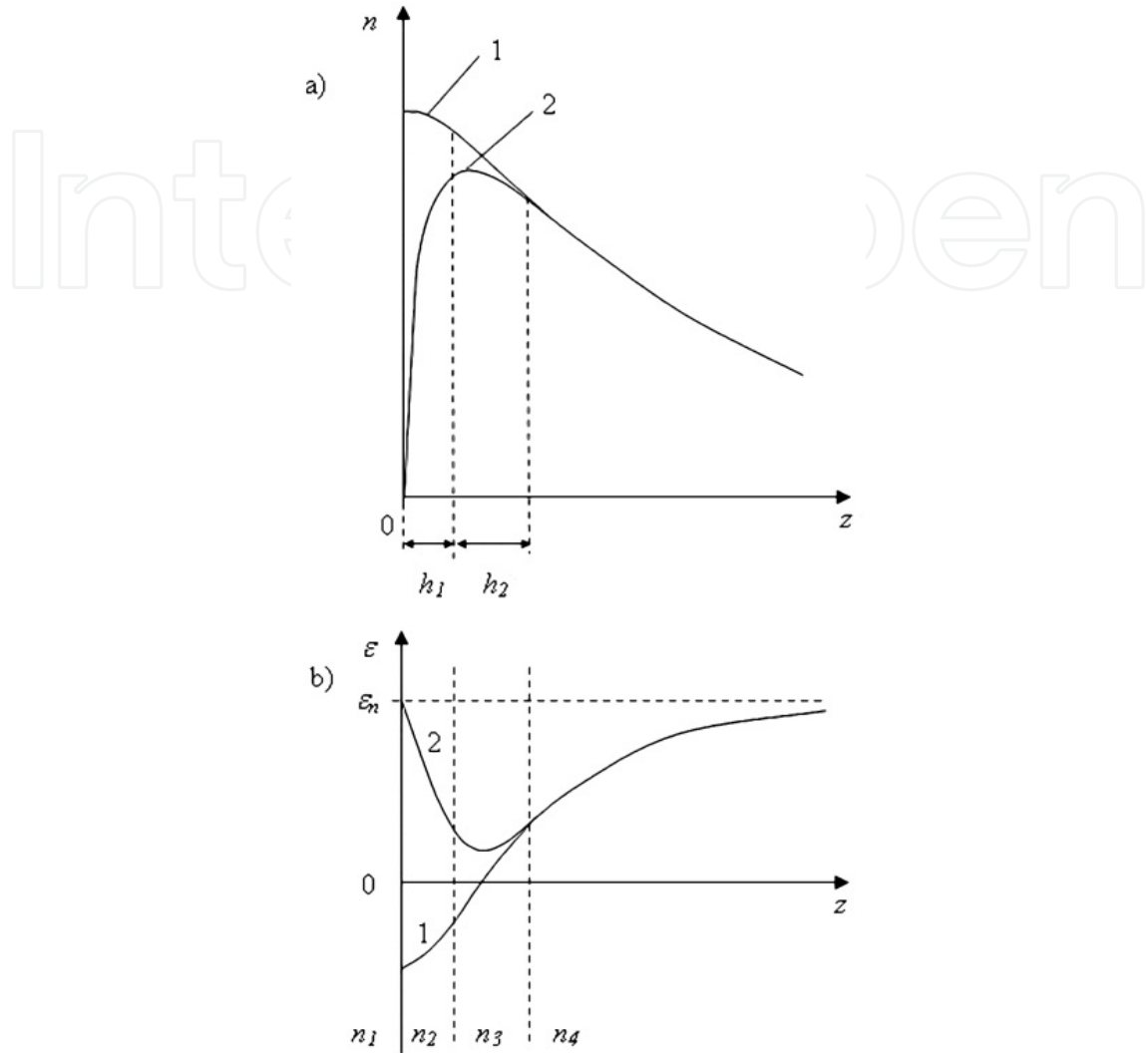


Figure 11. Schematic distribution of the electrons concentration in a semiconductor under the femtosecond laser pulse action (a) and the corresponding distribution of the dielectric permeability (b) for different emissions; n_1, n_2, n_3, n_4 - effective refractive indices of the layers as they are alternating along the coordinate z

In addition, it is necessary to provide a certain minimum thickness of the waveguide layer at a given frequency. If action of laser radiation results in formation of a layer with a refractive index n_3 and closer to surface a layer of thickness h_1 with a refractive index n_2 provided $n_2 > n_3 > n_1$, then [7]

$$h_{\min} \approx \frac{\lambda}{2\pi\sqrt{n_2^2 - n_3^2}} \arccos \sqrt{\frac{n_2^2 - n_3^2}{n_2^2 - n_1^2}}. \quad (22)$$

In particular, for silicon at a wavelength of $1.25 \mu\text{m}$ the minimum thickness of the waveguide layer is $h_{\min} \sim 70 \text{ nm}$ according to expression (22).

Let us consider the calculated spatial distribution of the silicon dielectric permeability under the femtosecond laser pulse action (see Fig. 10) in terms of the possible conversion of the incident light into surface plasmon-polaritons and waveguide modes. The surface polariton excitation requires transition of the semiconductor surface into a metal-like state, while formation of a dynamic optically-layered structure with a certain minimum thickness of the waveguide layer is necessary for the excitation and propagation of waveguide modes.

As follows from the numerical model (Fig. 10, curves 1-2) in case of relatively low emission a metal-like layer is formed at the surface. Within the layer thickness is about 50-60 nm dielectric permeability becomes negative. This provides the conditions for excitation of surface plasmon-polaritons (TM-type SEW), which is confirmed experimentally by formation of the microstructures perpendicularly to the polarization vector.

If emission rate is high as in case of thermo-emission (Fig. 10, curve 3) an optically layered structure is formed. Although the dielectric permeability does not change its sign, excitation of waveguide modes is possible.

Combination of both photo- and thermal-emission (Fig. 10, curve 4) results in formation of a dielectric layer of thickness ~ 60 nm and a metal-like layer of thickness about 40 nm. The refractive index of this dielectric layer is higher than both the refractive index of the air on one interface, and the refractive index of the metal-like layer on the other interface. Presence of such an optical structure enables excitation of waveguide mode, which results in the formation of periodic relief, which is parallel to the polarization vector on the incident radiation (see Fig. 6, right).

The above consideration showed that multiphoton emission and thermionic emission noticeably vary the optical properties of a semiconductor during a femtosecond pulse action. In particular, layer with different optical properties is formed at the surface and enables excitation of either surface polaritons or waveguide modes in the semiconductors. The considered model allows one to qualitatively and quantitatively interpret available experimental data. This approach allows one to use experimentally observed surface microstructures as relatively simple means of investigation of dynamics of the semiconductor surface properties under femtosecond action.

4. Conclusion

The results of numerical simulation have shown that influence of emission processes on the electron gas temperature and lattice temperature of metals is negligible. Therefore, the emission can be neglected when assessing the parameters of metals processing by femtosecond laser pulse, which simplifies the numerical calculations.

The Coulomb explosion occurrence in metals requires high-power incident radiation, which is impossible for the real exposure conditions.

However, in semiconductors both types of extrinsic emission noticeably change distribution of dielectric permeability near surface providing conditions for excitation of surface polaritons or waveguide modes depending on laser power magnitude.

The proposed method allowed to estimate the cross sections of multiphoton absorption in metals. For example, for metals absorption cross section: $\sigma_1=10^{-17}\text{cm}^2$ for one-photon absorption, $\sigma_2=10^{-28}\text{cm s}$ for two-photon absorption, $\sigma_3=10^{-61}\text{cm}^3\text{s}^2$ for three-photon absorption.

Author details

Roman V. Dyukin, George A. Martsinovskiy, Olga N. Sergaeva, Galina D. Shandybina, Vera V. Svirina and Eugeny B. Yakovlev
*Department of Laser-Assisted Technologies and Applied Ecology,
 National Research University of Information Technologies, Mechanics and Optics,
 Saint-Petersburg, Russia*

Acknowledgement

This work was supported by grants of RFBR 09-02-00932-a, 09-02-01065-a and State Contract No P1134.

5. References

- [1] Korte F., Nolte S., Chichkov B.N., Bauer T., Kamlage G., Wagner T., Fallnich C., Welling H. (1999) Far-Field and Near-Field Material Processing with Femtosecond Laser Pulses. *Appl. Phys. A*, 69 [Suppl.]: S7–S11.
- [2] Vorobyev D.Y., Guo C.L., (2010) Metallic Light Absorbers Produced by Femtosecond Laser Pulses. *Advances in Mechanical Engineering*, 2010: 1-5.
- [3] Chimmalgi A., Grigoropoulos C.P., Komvopoulos K. (2005) Surface Nanostructuring by Nano-Femtosecond Laser Assistant Force Microscopy. *App. Phys.* 97: 1043191 - 104319112.
- [4] Myers R.A., Farrell R., Karger A.M., Carey J.E., Mazur E. (2006) Enhancing Near-Infrared Avalanche Photodiode Performance by Femtosecond Laser Microstructuring. *Appl Opt.* 45(35): 8825-31.
- [5] Etsion I. (2005) State of the Art in Laser Surface Texturing. *J. of Tribology*, 127(1): 248-253.
- [6] Oktem B., Kalaycioglu H., Erdoğan M., Yavaş S., Mukhopadhyay P., Tazebay U. H., Aykaç Y., Eken K., Ilday F. Ö. (2010) Surface Texturing of Dental Implant Surfaces with an Ultrafast Fiber Laser. in *Conference on Lasers and Electro-Optics, OSA Technical Digest (CD) (Optical Society of America, 2010)*, JTuD15.
- [7] Libenson M.N. (2007) [Laser-Induced Optical and Thermal Processes in Solids and Their Mutual Influence]. Saint-Petersburg: Nauka. 423 p. (in Russian)
- [8] Libenson M.N. (2001) Non-Equilibrium Heating and Cooling of Metals Under Action of Super-Short Laser Pulse. *Proc. SPIE.* 4423: 1–7.
- [9] Carey J.E., Crouch C.H., Mazur E. (2003) Femtosecond-Laser-Assisted Microstructuring of Silicon Surfaces. *Optics&Photonics News.* 14(2): 32-36.
- [10] Shimosuma Y., Kazansky P.G., Qin J.R., Hirao K. (2003) Self-Organized Nanogratings in Glass Irradiated by Ultrashort Light Pulses. *Phys. Rev. Lett.* 91: 247405-247409.

- [11] Kudryashov S.I., Emel'yanov V.I. (2001) Electron gas compression and Coulomb explosion in the surface layer of a conductor heated by femtosecond laser pulse. *JETP Lett.* 73(12): 666-670.
- [12] Evans R., Badger A.D., Fallies F., Mahdih M., Hall T.A., Audebert P., Geindre J.-P., Gauthier J. C., Mysyrowicz A., Grillon G., Antonetti A. (1996) Time- and Space-Resolved Optical Probing of Femtosecond-Laser-Driven Shock Waves in Aluminum. *Phys. Rev. Lett.* 77(16): 3359-3362.
- [13] Del Fatti N., Arbouet A., Vall'ee F. (2006) Femtosecond Optical Investigation of Electron-Lattice Interactions in an Ensemble and a Single Metal Nanoparticle. *Appl. Phys. B.* 84: 175-181.
- [14] Chen. L.M., Zhang J., Dong Q.L., Teng H., Liang T.J., Zhao L.Z., Wei Z.Y. (2001) Hot Electron Generation Via Vacuum Heating Process in Femtosecond Laser-Solid Interactions. *Phys. of Plasmas.* 8(6): 2925-2929.
- [15] Kaganov M.I., Lifshitz I.M., Tanatarov L.V. (1956) [Relaxation between Electrons and Lattice]. *J. Exp. Theor. Phys.* 31(2): 232-237. (in Russian)
- [16] Anisimov S.I., Kapeliovich B.L., Perelman T.L. (1974) [Electron Emission from Metal Surfaces Exposed to Ultrashort Laser Pulses]. *J. Exp. Theor. Phys.* 39(2): 375-377. (In Russian)
- [17] Anisimov S.I., Benderskii V.A., Farkas G. (1977) Nonlinear Photoelectric Emission from Metals Induced by a Laser Radiation. *Soviet Physics Uspekhi.* 20(6): 467-488.
- [18] Delone N.B. (1989) [Interaction of Laser Beam with Matter. The course of lectures]. Moscow: Nauka. 289 p. (In Russian)
- [19] Kato S., Kawakami R., Mima K. (1991) Nonlinear Inverse Bremsstrahlung in Solid-Density Plasmas. *Phys. Rev. A.* 43(10): 5560-5567.
- [20] Wang X.Y., Downer M.C. (1992) Femtosecond Time-Resolved Reflectivity of Hydrodynamically Expanding Metal Surfaces. *Optics Letters.* 17(20): 1450-1452.
- [21] Rethfeld B., Kaiser A., Vicanek M., Simonc G. (2001) Nonequilibrium Electron and Phonon Dynamics in Solids Absorbing a Subpicosecond Laser Pulse. *Proc. SPIE.* 4423: 250-261.
- [22] Rethfeld B., Kaiser A., Vicanek M., Simon G. (2002) Ultrafast Dynamics of Nonequilibrium Electrons in Metals under Femtosecond Laser Irradiation. *Phys.l Rev. B.* 65: 214303-214313.
- [23] Ashcroft N.W., Mermin N.D. (1976) *Solid State Physics.* New York: Holt, Rinehart, and Winston. 826 p.
- [24] Bulgakova N.M., Rosenfeld A., Ehrentraut L., Stoian R., Hertel I.V. (2007) Modeling of Electron Dynamics in Laser-Irradiated Solids: Progress Achieved Through a Continuum Approach and Future Prospects. *Proc. SPIE.* 6732: 673208-673223.
- [25] Zobotnov S.V., Ostapenko L.A., Golovan L.A., Shandybina G.D., Timoshenko V.Yu., Kashkarov P.K. (2005) Third Optical Harmonic Generation of Silicon Surfaces Structured by Femtosecond Laser Pulses. *Proc. SPIE.* 6161: 0J1-0J5.
- [26] Ostapenko I.A., Zobotnov S.V., Shandybina G.D., Golovan L.A., Chervyakov A.V., Ryabchikov Yu.V., Yakovlev V.V., Timoshenko V.Yu., Kashkarov P.K. (2006) Micro- and Nanostructuring of Crystalline Silicon Surface under Femtosecond Laser Pulses. *Bulletin of RAS: Physics.* 70: 1503-1506.